Amplitude-corrections for randomly distributed heterogeneities above a target reflector

C. Sick, T. M. Müller, S. A. Shapiro, and S. Buske

email: *sicky@geophysik.fu-berlin.de*

keywords: *AVO, scattering attenuation, reflection coefficient*

ABSTRACT

In seismic reflection experiments, the reflected wave is strongly influenced by heterogeneities in the reflector overburden. Thus, the amplitude of the reflected wave decreases due to scattering attenuation. This effect must be taken into account when generating seismic images of the reflector as well as for calculating the reflection coefficients. Using the generalized O'Doherty Anstey formalism for 2-D and 3-D random media it is possible to correct this transmission losses due to scattering. We apply this correction method to synthetic data for 2-D randomly heterogeneous media. AVO/AVA analysis of the corrected data yields more reliable estimations of reflection coefficient.

INTRODUCTION

Accurate estimations of reflection coefficients are of great importance for reservoir characterization as well as for seismological studies of crystalline-crustal structures. In deep seismic soundings, assessments of reflection coefficients are generally obtained by calculating the ratio of reflected to incident amplitudes. In traditional AVO/AVA-processing schemes the amplitudes of the raw data are used, while in modern AVO/AVA analysis the use of the amplitudes of migrated sections is common practice. So far, in conventional procedures geometrical spreading was taken into account, but the transmission losses due to scattering at isomorphic small scale heterogeneities within the overburden have been ignored.

It is well known that scattering attenuation and dispersion influence strongly the amplitudes of waves propagating through an heterogeneous medium. These transmission losses due to scattering cause an underestimation of the reflection coefficients. Widmaier et al. (1996) have shown how to compensate for these effects in layered media. They included this compensation into an amplitude-preserving Kirchhoff migration scheme, but they pointed out, that it can also be used in traditional AVO/AVA- processing schemes shown e.g. by Castagna (1993). Another correction strategy was proposed e.g. by Wapenaar and Herrman (1996). In respect of the work of Widmaier et al., we use the traditionally way here. This study proposes a method that compensates

the scattering attenuation effects due to random isomorphic heterogeneities, so that it is possible to obtain a more reliable estimation of reflection coefficients.

First, we outline the scattering attenuation description as proposed in a work of Müller and Shapiro (2001) about pulse propagation in heterogeneous media. Thereafter, using synthetic seismograms of a shot gather, we illustrate how to improve amplitude processing in order to compensate for the effect of scattering attenuation. This is done by means of two numerical examples. The first refers to the scaling typical for reflection seismology of a subducting plate involving crystalline rocks. The second example refers to a the scaling typical for exploration seismology, where the overburden of a target reflector is heterogeneous. Original and corrected synthetic AVA-curves for both examples are then compared to results for the corresponding homogeneous reference models. Finally, in order to suppress random fluctuations of AVA curves, we perform the same AVA-processing scheme using more than one shot and discuss the results in comparison with those for a single shot.

THEORY OF SCATTERING ATTENUATION

Theoretical methods to describe the pulse propagation and to quantify scattering attenuation include the meanfield theory using the Born approximation or the traveltime-corrected meanfield formalism developed by Sato (1982) and Wu (1982). The meanfield theory overestimates scattering attenuation, while the traveltime-corrected meanfield formalism excludes large wavenumbers so that scattering at large-scale heterogeneities is not taken into account. Additionally, it requires a heuristically chosen cut-off wavenumber which can be only determined by numerical tests.

Primary wavefields can be described by the generalized O'Doherty-Anstey formalism in single realizations of 1-D random media Shapiro and Hubral (1999). Based on the Rytov and Bourret approximations Müller and Shapiro (2001) described the seismic primary propagation in single realizations of 2-D and 3-D random media. Using the causality principle, Müller et al. (2001) extended this formalism to a broad frequency range. Due to sound analogies it can be understood as an extension of the O'Doherty-Anstey theory to 2-D and 3-D random media. In the case of a point source excitation in 2-D we find the following approximation for the Green's function from this theory:

$$G(t,L) = \frac{1}{2\pi}\int_{-\infty}^{\infty} d\omega\, e^{-\alpha L + i\varphi L} e^{-i\omega t}\,, \tag{1}$$

where

$$\begin{aligned}\alpha(\omega, L, a, \sigma^2) \;\approx\; & 2\pi k^2 \int_0^{\infty} d\kappa\, \Phi^{2D}(\kappa)\Bigg[H(2k-\kappa) - \\ & \frac{\cos(\kappa^2 L/4k)\, FC(\sqrt{\kappa^2 L/2\pi k})}{\sqrt{\kappa^2 L/2\pi k}} + \\ & \frac{\sin(\kappa^2 L/4k)\, FS(\sqrt{\kappa^2 L/2\pi k})}{\sqrt{\kappa^2 L/2\pi k}}\Bigg]\end{aligned} \tag{2}$$

is the scattering attenuation coefficient and

$$\begin{aligned}\varphi(\omega, L, a, \sigma^2) \;\approx\; & k + 2\pi k^2 \int_0^\infty d\kappa\, \Phi^{2D}(\kappa) \left[\frac{2kH(2k-\kappa)}{\sqrt{\kappa^2 - 4k^2}} - \right. \\ & \frac{\sin(\kappa^2 L/4k)\, FC(\sqrt{\kappa^2 L/2\pi k})}{\sqrt{\kappa^2 L/2\pi k}} + \\ & \left. \frac{\cos(\kappa^2 L/4k)\, FS(\sqrt{\kappa^2 L/2\pi k})}{\sqrt{\kappa^2 L/2\pi k}} \right] \end{aligned} \tag{3}$$

denotes the phase increment. In equations (1)-(3) $k = \frac{\omega}{c_0}$ denotes the wavenumber, where c_0 is the constant background velocity, resulting from the averaged squared slowness, and L represents the travel distance. $\Phi^{2D}(\kappa)$ is the fluctuation spectrum which contains the second-order statistics of the medium's fluctuations, i.e. the variance σ^2 of the P-wave (S-wave) velocity in rocks and the correlation length a. H denotes the Heaviside step function. The functions FC and FS denote the Fresnel cosine and sine integrals, respectively. The validity range of the Green's function (1) in terms of the wave parameter $D = 2L/(ka^2)$ is

$$\max\left\{\frac{\lambda}{a}, \frac{\lambda^2}{a^2}\right\} < \pi D < \left(\frac{L}{a}\right)^2 \min\left\{1, \frac{\lambda}{a}\right\}, \tag{4}$$

where λ denotes the wavelength. Note that equation (1) is also restricted to the weak wavefield fluctuation regime. The formula for the scattering attenuation coefficient in the 3-D case could be calculated by multiplying the integral in equation (2) with another π and the bracket term with κ. We emphasize that the Green's function (1) is suitable to estimate single realizations of seismograms. More precisely, equation (1) describes maximum probable primaries. No averaging must be applied to the wavefield. In principle, equations 1- 3 can be used to correct the wavefield for amplitude as well as for velocity dispersions and traveltime shift effects of the elastic scattering in the overburden. In this paper we restrict ourself to the correction of the impact of attenuation effect, as the most significant scattering effect in disturbance of amplitudes.

The transmission losses are characterized by the scattering attenuation coefficient (2). According to equation (1), the transmissivity is approximately given by

$$T(L, \omega_0) \approx e^{-\alpha(L,\omega_0)L}, \tag{5}$$

where ω_0 is the dominant frequency of the transmitted wavelet. Regarding equation (2) it is clear that informations about the statistical properties of the medium have to be known. If near-surface studies are performed, the statistical medium attributes can be obtained by using well-log data. For deeper investigations, or in the case of deep reflection profiling of the lithosphere, these properties have to be determined from statistical analysis of teleseismic or local seismicity wavefield fluctuations (see e.g. Wu and Flatté, 1990).

EXAMPLE FROM REFLECTION SEISMOLOGY: A SUBDUCTING PLATE

In our first example we used a model, which scaling is based on a section of the ANCORP96 profile in the Central Andes, South America. It illustrates a dipping reflector at a depth of about 60-70 km ("the subducting plate") overlaid by a layer with randomly distributed velocity and density fluctuations (see Figure 1 for details). We modeled wave propagation by using a 2-D finite-difference staggered grid scheme for the elastodynamic wave equation (Saenger et al., 2000). The heterogeneous overburden consists of statistically isotropic velocity fluctuations characterized by an exponential autocorrelation function like $B(r) = \sigma^2 e^{-\frac{|r|}{a}}$. Thereby a standard deviation of $\sigma = 1.5\%$ and a correlation length of $a = 1$ km are chosen, r represents the spatial distance. Furthermore, the constant P-wave velocity in the part of the model below the reflector is $8km/s$ and in the heterogeneous part the constant background velocity is $6km/s$. S-wave velocity is given by $v_s = \frac{v_p}{\sqrt{3}}$, the density by an approximation of the Nafe-Drake (see e.g. Ludwig et al., 1970) relation $\rho = (1.755 + 0.155\frac{v_p}{1000}) \cdot 1000[kg/m^3]$. Starting from a point source at 80km (see Figure 1), the waveforms are recorded with 200 receivers over an offset range of about 20km. Thus, the resulting travel distances are between 120km and 140km.

The right hand side of Figure 1 shows an example of some of the computed synthetic seismograms. The magnification of the reflected P-waves in Figure 1 indicates that the amplitude decreases with increasing travel distance. This amplitude decrease is mainly caused by geomet-

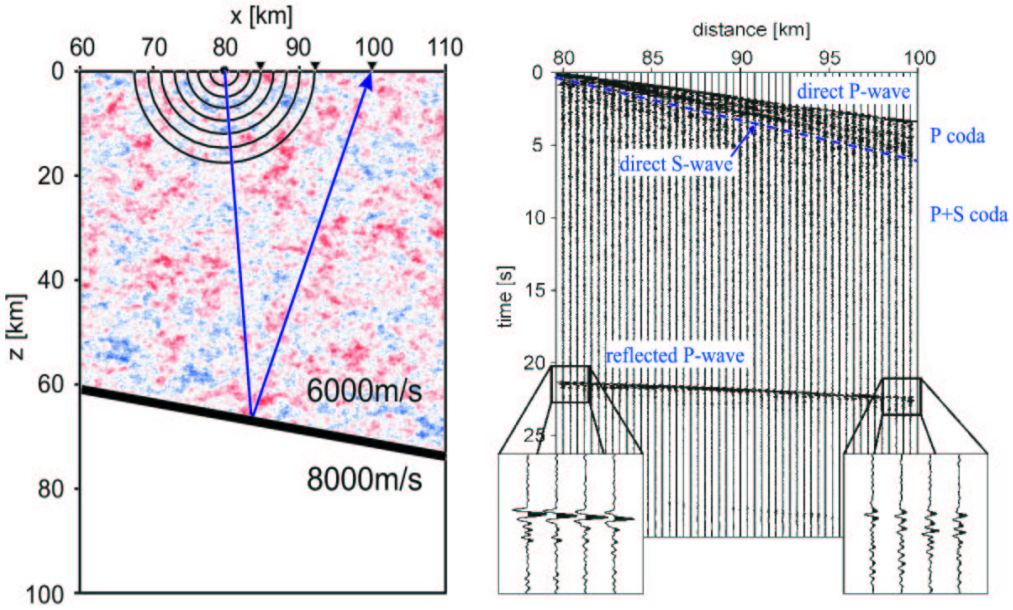

Figure 1: left: Model of a dipping reflector. The heterogeneous overburden is determined by a constant background P- velocity of $6km/s$. The S-velocity is about $3.5km/s$ and the mean density is $2700kg/m^3$. Below the reflector the constant P-velocity is $8km/s$, the S-velocity is about $4.6km/s$ and the density is $3000kg/m^3$. The point source is located at $x = 80km$ and 200 receivers are placed between $80km$ and $100km$. Right: Shot gather (z-component). The zooms shows some reflected p-wave amplitudes at short offsets (left) and large offsets (right).

rical spreading, but its significant amount is also due to scattering. Later, synthetic sections will show that the effect of scattering attenuation is smaller than the effect of geometrical spreading but it also has to be taken into account to prevent an underestimation of the reflection coefficient.

For computing the reflection coefficient, the amplitudes of the direct and the reflected waves are used. Using the traditional AVA-processing scheme as described by Castagna, we picked the x- and z-components of both waves and performed a vector-addition of the components. After this step, we corrected the amplitudes for geometrical spreading. Usually, this correction for geometrical spreading is the last step of the processing before calculating the reflection coefficient, but we additionally introduced a travel distance- and frequency-dependent scattering correction as a new step in the amplitude processing scheme. For this correction, the amplitudes have to be multiplied with the reciprocal transmissivity $T^{-1}(L, \omega_0) = e^{\alpha(L,\omega_0)L}$ (see also equation 5) before evaluating the reflection coefficient $R = \frac{A_{incident}}{A_{reflected}}$ as a function of angle of incidence (or offset). We calculated the amplitude spectrum of the reflected wave to get the dominant frequency (see Figure 2). The amplitude spectrum indicates a dominant frequency between 6.4Hz and 8.4Hz. Figure 3 illustrates the reciprocal transmissivity for several frequencies depending on travel distance for our model. The black line represents the reciprocal transmissivity for a frequency of about 7.4Hz. The plot shows that the reciprocal transmissivity is not strongly sensitive to the frequency in the interval between 6.4Hz and 8.4Hz. We chose the mean value (7.4Hz) as our dominant frequency.

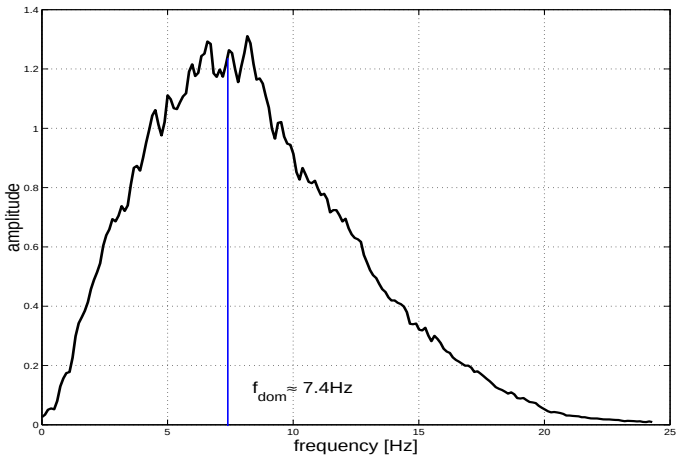

Figure 2: Amplitude-spectrum of the reflected wave. The dominant frequency is approximately $f_{dom} \approx 7.4Hz$.

By means of one trace with offset $5600m$, Figure 4 shows the influence of the correction of the transmission losses due to scattering. The black dashed line represents the uncorrected trace, while the solid grey line shows the trace which has been corrected for the above mentioned scattering losses. It is obvious, that the discrepancy between the corrected and the uncorrected amplitude is quite significant. In this example the difference between corrected and uncorrected amplitude is about 30%.

This difference exists for all reflected amplitudes. So, the comparison between corrected and uncorrected amplitudes for all offsets results in an underestimation of about 30%, if the correction

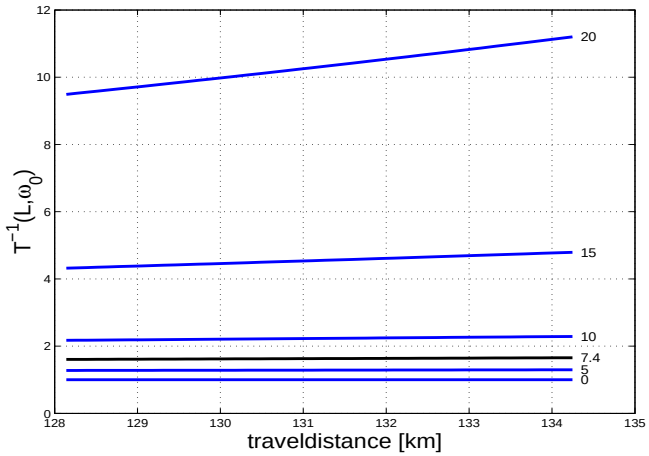

Figure 3: Reciprocal transmissivity versus travel distance for frequencies from 0Hz (bottom) to 20Hz (top) in steps of 5Hz (blue lines). The black line shows the values for our dominant frequency 7.4Hz.

is not used. Thus, this error occurs also in the estimation of the reflection coefficient. Our computed corrected and uncorrected reflection coefficients in combination with the theoretical value for a homogeneous reference model are shown in Figure 5. To calculate these theoretical values we used an explicit equation for P-P reflectivity derived from the Zoeppritz equations by Aki and Richards (see also Castagna, 1993), which is valid for small changes in layer properties.

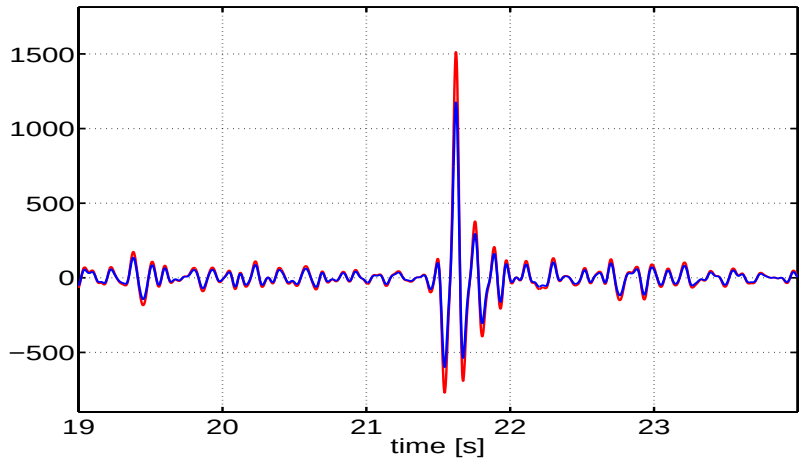

Figure 4: Part of the uncorrected (blue line) and the corrected (red line) reflected trace recorded at 5600m offset.

Working with one shot and fitting the R_{PP} in both cases (uncorrected and corrected) by a straight line (Figure 5a), a significant improvement can be observed after the correction: The grey line corresponding to the corrected reflection coefficients agrees reasonably well with the black curve corresponding to the homogeneous reference model. Thus, the proposed amplitude processing indeed corrects for scattering attenuation due to small scale heterogeneities (in respect

to the travel distance) in the reflector overburden. Without the scattering attenuation correction significantly smaller reflection coefficients are obtained. It can be seen that the proposed correction also improves the general behavior of the reflection coefficient. However, the relative fluctuations of R_{PP} remain uncompensated. A strategy to reduce these fluctuations is following.

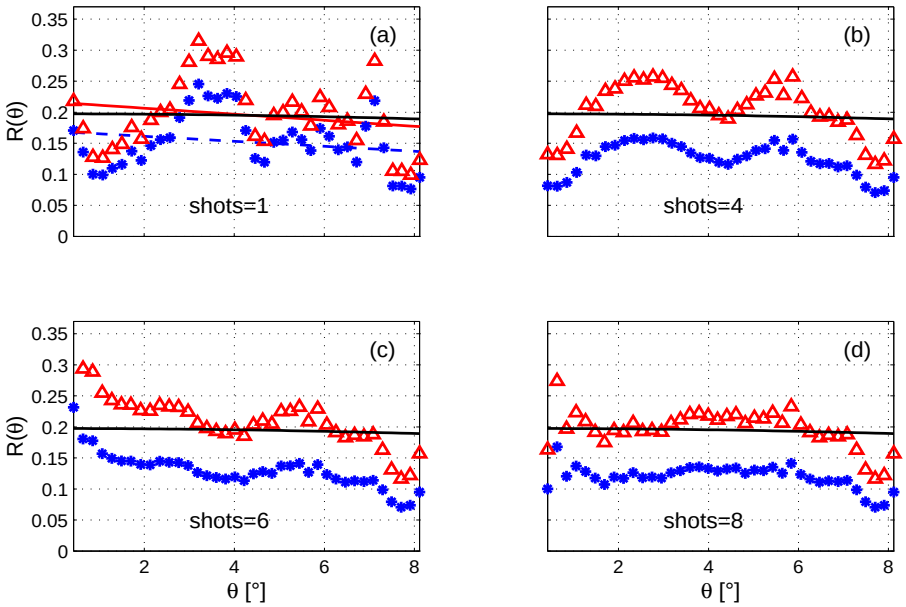

Figure 5: Variation of reflection coefficient by stepwise added shot points for a model of a subducting plate. (a) The dashed blue line and the red solid represent the linear fits for corrected and uncorrected R_{PP}, respectively. (a-d) Blue points: Mean values of the uncorrected R_{PP}, red triangles: Mean values of the corrected R_{PP}, black solid: R_{PP} in the homogeneous reference model.

Figure 5a shows that due to interaction with random heterogeneities in the overburden the reflection coefficient R_{PP} is not only decreased but exhibits strong fluctuations. Thus, the interpretation of the AVO/AVA behavior is still difficult. We propose to reduce these fluctuations by using more than one shot. To demonstrate this, we consider eight shot points with distances of one correlation length ($1km$) from each other, whereas the first shot point is the same as in the first experiment. Regarding same offsets of the different shots, the reflected rays pass through different heterogeneities, so on an average the fluctuations should be decreased. After picking the direct and reflected amplitudes of every trace, we calculated the reflection coefficients for each shot and corrected them for transmission losses in the same way as described above. Then we assigned the computed R_{PP} values to their corresponding angles and averaged over the shots. Moreover, the stepwise reduction of the fluctuations of the reflection coefficient with increasing number of shot points involved into the averaging is illustrated in Figure 5b-5d. The mean values of R_{PP} for same angles for 4,6 and 8 shots are shown in this figure. A comparison of the result with eight shots to that with one (Figure 5a) illustrates the improvement when many shots are used: The use of the shot averaging reduces the fluctuations of R_{PP} obviously. Now an interpretation of the AVA behavior becomes possible. Because of the chosen geometry the reflection

coefficients outside the interval $[1.2°, 7°]$ are not averaged with as much values as the rest of the points. This explains, why the fluctuations are still large there.

EXAMPLE FROM EXPLORATION SEISMOLOGY: A PLANE HORIZONTAL REFLECTOR WITH A HETEROGENEOUS OVERBURDEN

In this example we construct a model with a plane target reflector, which is overlaid by random heterogeneities. The depth of the reflector is supposed at 1.5km. Here, 700 receivers are distributed over an offset range of 2.8km, so that the maximum travel distance is about 4km. We choose a correlation length of $a = 40$ m and a standard deviation of $\sigma = 3\%$. For this example, the heterogeneous overburden is determined with a constant background velocity of $3km/s$ and the homogeneous part below the reflector with a constant P-wave velocity of $4km/s$. S-wave velocity and density are calculated as shown in the first example. The dominant frequency is about 47Hz. The strategy to calculate the reflection coefficient for this example is the same as described above.

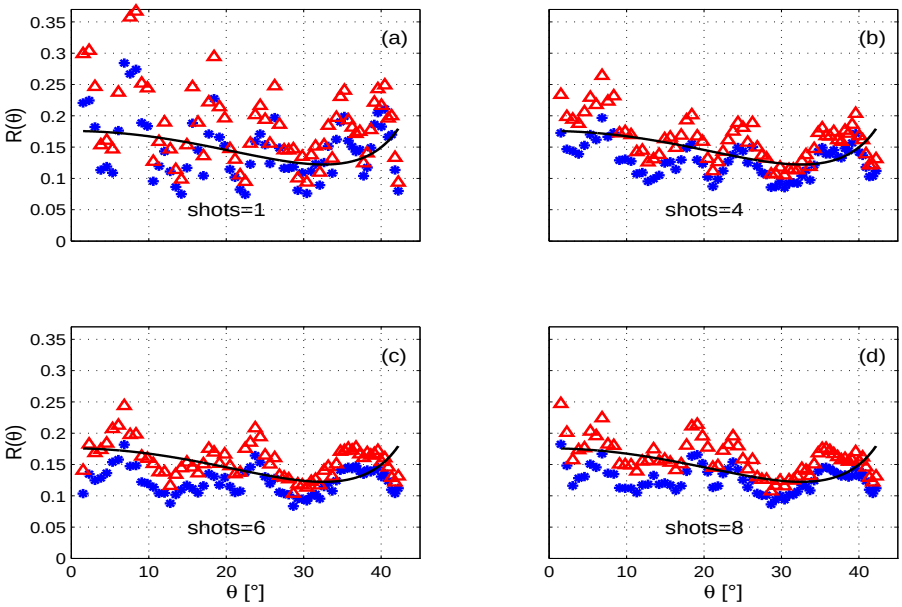

Figure 6: Reflection coefficient for a model of a plane horizontal reflector with a heterogeneous overburden. (a-d) Blue points: mean values of the uncorrected R_{PP}, red triangles: mean values of the corrected R_{PP}, black solid: R_{PP} in the homogeneous reference model.

Figure 6 shows the results of the R_{PP} calculations. As well as in the reflection seismology example, we noticed an improvement of R_{PP} after using the correction. However, the difference between corrected and uncorrected reflection coefficient is not as large as in the example above. For small offsets this difference is more significant than for large offsets. This is caused by the small discrepancy between large offsets O and travel distances L, so that the exponential terms in the correction formula $R_{PP} = \frac{A_r e^{\alpha(L,\omega_0)L}}{A_i e^{\alpha(O,\omega_0)O}}$ practically cancel out.

The influence of the transmission losses due to scattering can obviously be seen in Figure

6b-6d. At first glance, regarding Figure 6a, the computed results with one shot gather seem not deal with the corresponding theoretical R_{PP} curve at all. Reliable estimation and interpretation of AVA behavior is not possible until more than one shots are used. Figure 6d shows, that the underestimation for small offsets is about 25% while for large offset it is around 15% when the correction is not used.

CONCLUSIONS

Normally, AVO-analysis is done by using geometrical spreading corrections only. Here we show that scattering attenuation due to small scale heterogeneities (in respect to travel distance) in the reflector overburden significantly influences the amplitudes of reflected P-waves. This study demonstrates by means of two numerical examples how to compensate for this effect. For both examples, one referring to a deep seismic sounding experiment, and the other to the scale of a typical seismic exploration experiment, we obtain an improvement of calculated reflection coefficients after using the correction for transmission losses due to scattering. Nevertheless, the fluctuations of the reflection coefficient are quite strong in both cases when only one shot gather is used. Taking into account the seismograms from more shots, the calculated and corrected angle-dependent reflection coefficient resembles the situation when there were no velocity fluctuations in the overburden. Thus, using our method to compensate for the transmission losses makes it possible to estimate reflection coefficients more reliable and to reveal the actual AVA behavior in complex structures.

ACKNOWLEDGMENTS

The authors thank the sponsors of the Wave Inversion Technology Consortium (WIT) and the SFB 267 for their support. Furthermore many thanks to the Konrad-Zuse-Zentrum für Informationstechnik Berlin which provide their CRAY T3E to the authors to calculate the numerical simulations.

REFERENCES

Aki, K. and Richards, P. G. (1980). *Qantitative seismology: Theory and methods*. Freeman, New York.

Castagna, J. P. (1993). Avo analysis-tutorial and review,. In Castagna, J. P. and Backus, M. M., editors, *Offset dependent reflectivity: Theory and practice of AVO analysis*, pages 3–36. Soc. Expl. Geophys.

Ludwig, J., Nafe, J., and Drake, C. (1970). Seismic refraction. In Maxwell, A., editor, *The Sea*, volume 4, pages 53–84. Wiley, New York.

Müller, T. M. and Shapiro, S. A. (2001). Most probable seismic pulses in single realizations of two- and three-dimensional random media. *Geophys. J. Int.*, 144(01):83–95.

Müller, T. M., Shapiro, S. A., and Sick, C. M. A. (2001). Most probable ballistic waves in

random media: A weak fluctuation approximation and numerical results. *Waves Random Media, accepted*.

Saenger, E. H., Gold, N., and Shapiro, S. A. (2000). Modeling the propagation of elastic waves using a modified finite-difference grid. *Wave Motion*, 31:77–92.

Sato, H. (1982). Amplitude attenuation of impulsive waves in random media based on traveltime corrected mean wave formalism. *J. acoust. Soc. Am.*, 71:559–564.

Sato, H. and Fehler, M. (1998). *Seismic wave propagation and scattering in the heterogeneous earth*. AIP press, New York.

Shapiro, S. A. and Hubral, P. (1999). *Elastic waves in random media*. Springer, Berlin.

Wapenaar, C. and Herrman, F. (1996). True amplitude migration taking fine-layering into account. *Geophysics*, 61:795–803.

Widmaier, M., Shapiro, S. A., and Hubral, P. (1996). Avo correction for scalar waves in the case of a thinly layered reflector overburden. *Geophysics*, 61:520–528.

Wu, R.-S. (1982). Mean field attenuation and amplitude attenuation due to wave scattering. *Wave Motion*, 4:305–326.

Wu, R.-S. and Flatté, S. M. (1990). Transmission fluctuations across an array and heterogeneities in the crust and upper mantle. *PAGEOPH*, 132:175–192.